International Conference on Space Optics—ICSO 2018

Chania, Greece

9–12 October 2018

Demonstration of strain independent temperature measurements using optical PM-FBG sensors for ground testing of satellite panels

Selwan Ibrahim

Raymond McCue

John O'Dowd

Martin Farnan

et al.

Demonstration of Strain Independent Temperature Measurements Using Optical PM-FBG Sensors for Ground Testing of Satellite Panels

Selwan K. Ibrahim*[a], Raymond McCue[a], John A. O'Dowd[a],
Martin Farnan[a], Devrez M. Karabacak[b]
[a]FAZ Technology Ltd., 9C Beckett Way, Park West Business Park, Dublin 12, Ireland;
[b]Fugro Technology BV Veurse Achterweg 10, 2264 SG Leidschendam, The Netherlands

ABSTRACT

Photonically wired spacecraft panels have been demonstrated within a recent ESA ARTES project by integrating mechanically packaged fiber Bragg grating (FBG) based optical temperature sensors into a honeycomb satellite test panel. Replacing electrical sensors with optical fiber sensors for testing satellites should have the advantage of reducing the harness mass and AIT. Fiber optic sensing also comes with clear benefits including immunity to electromagnetic interference and the capability of supporting arrays of sensors on a single fiber. However, standard FBG based temperature sensors are sensitive to both strain and temperature and in order to measure both strain and temperature simultaneously, two FBG sensors are required. An alternative solution using birefringent FBGs inscribed in Polarization Maintaining (PM) fiber (PM-FBG) in combination with high precision optical interrogators offers the same capabilities of standard FBG based optical sensors with high accuracy measurements, and can simultaneously measure both strain and temperature using only one sensor. PM-FBG sensors can also be multiplexed on a single fiber and therefore offer a simplified installation option by mounting them on the surface of the structure without the requirement for complex transducer packaging designs. With the support from an ESA GSTP project, we have developed an optical interrogator that measures PM-FBGs with high accuracy. The aim of the project is to demonstrate an optical strain independent temperature measurement system using PM-FBGs installed on a satellite test panel in atmospheric pressure and thermal vacuum environments with an operating temperature range from -20°C to + 80°C.

Keywords: Optical Sensing, Fiber Bragg Grating, FBG, Polarization, PM-FBG, Fiber Sensing, Optical Interrogator

1. INTRODUCTION

Today telecommunication satellite sensing systems require a complex wiring harness which leads to increased Assembly, Integration and Testing (AIT) effort, weight and overall cost[1, 2]. Traditional point-to-point wiring of electrical temperature sensors result in the vast size and weight of the harness. FBG based fiber optic sensors have been used recently to demonstrate temperature monitoring of a honey comb structure test panel designed for the small-GEO series satellite by HPS and OHB[3] as part of an ESA ARTES 5.1 project (Photonically Wired Spacecraft Panels) (4000111220/14/NL/AD). From this ARTES project, a demonstrator with three different panels, a large one (900 mm x 800 mm x 25 mm) and two smaller ones (280 mm x 280 mm x 25mm) were developed as shown in figure 1.

A FBG based temperature transducer was developed by OHB to enable the decoupling of strain and temperature both of which affect the Bragg wavelength shift of the grating[3]. However, this required packaging and calibration of each individual sensor which would add to the overall costs. FAZ Technology have developed within an ESA GSTP6.2 project (Development of a high precision interrogator to acquire data from birefringent FGB sensors, for ground testing of satellites), a birefringent interrogation system (FAZT I4_Bi) based on the FAZT I4 fiber sensing system using birefringent polarization maintaining FBGs (PM-FBG) to provide a strain independent temperature measurement system for one of the small test panels without the requirement of a custom transducer design to isolate strain. The main advantage of using PM-FBGs sensors is that they can offer simultaneous measurements of temperature and strain which simplifies the transducer design, packaging and mounting of the sensor. PM-FBG sensors can also be multiplexed on a single fiber and can offer simplified installation options by mounting them on the surface of the structure without the requirement for complex transducer packaging designs.
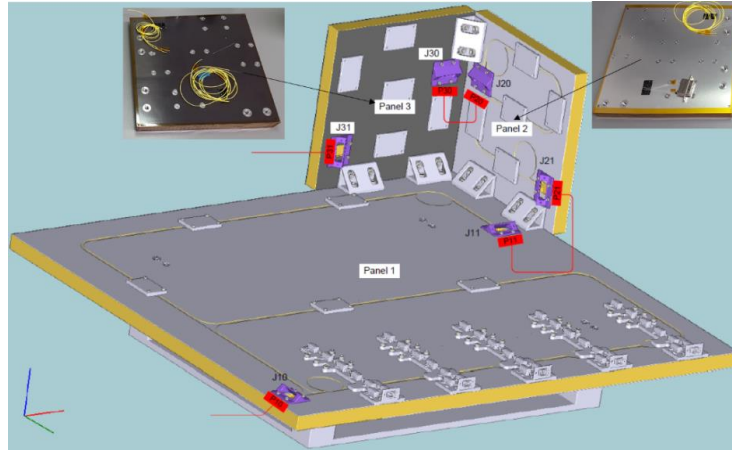
Figure 1. CAD model of the panel demonstrator showing an actual photo of the small panels manufactured by HPS for OHB as part of an ESA ARTES project.

2. EXPERIMENTAL SETUP

To demonstrate the PM-FBG technology, the PM-FBG based temperature sensors were mounted on the surface of the small test panel at certain positions as shown in figure 2 (left). The PM-FBG array was a PM-DTG (draw tower grating) type sensor array manufactured by FBGS using Ormocer coating. The FAZT I4_Bi tuneable laser interrogator platform is capable of measuring PM-FBGs with high precision in the sub pm range, surpassing today's state-of-the-art tunable laser interrogators. The schematic of FAZT I4_Bi interrogator and a PM-FBG array is shown in figure 2 (right).
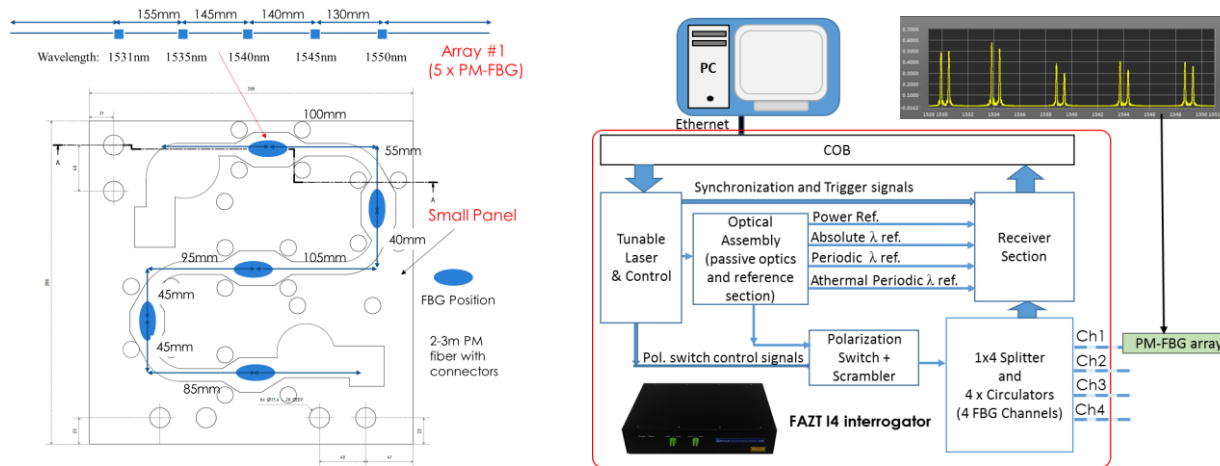
Figure 2. Layout of the 5 PM-FBG array installation on the small panel (left). Schematic of the FAZT I4_Bi interrogator system (right)

The interrogator has 4 channels and the polarization control section included a polarization switch and a high-speed scrambler based on a custom built phase modulator driven with sinusoidal RF signal at 800MHz. This configuration guaranteed the detection of the two orthogonal responses of the PM-FBGs in the sensor array at full scan rate (1 kHz sampling rate). The peak wavelength position of the two orthogonal FBG responses in addition to the wavelength difference between the two peaks contains all the required sensor information. Typically, the spacing between the peaks is in the order of 0.3 to 2nm and the temperature sensitivity for the wavelength difference of PM-FBGs are lower than standard FBGs (<1pm/°C).

The main objective of the experiments in this paper was to evaluate commercially available PM-FBG sensors for temperature measurements in the region of -20°C to +80°C in atmospheric and thermal vacuum (TV) conditions. The paper reports the results measured for two PM-DTG sensor arrays that were installed on a satellite honeycomb structure test panel (from HPS Portugal) as shown in figure 3.

Two main types of mounting techniques were used for two PM-DTG arrays. This involved installing one $5 \times$ PM-DTG array in a 0.7mm PTFE loose buffer tube and then attaching the PTFE tube on the panel at specific locations using Silicone (3140) RTV coating on 2 sensor locations, aluminium tape on 2 locations, and 1 sensor location left loose. The other $5 \times$ PM-DTG array measurements focused on 2 PM-DTGs directly glued on the panel using Silicone (3140) RTV coating, and 1 left loose. The test results also show the difference between different sensor mounting techniques on the panel and how they perform when temperature is cycled $>= 10$ times at atmospheric pressure. An accurate temperature probe (ISOTECH high precision electrical probe 935-14-61) located close to the sensors was used as a reference sensor for the temperature measurements at atmospheric pressure. For the TV tests, PT100 electrical sensors were used as shown in figure 3 (right). Table 1 lists all the PM-DTG optical sensors installed and measured on the panel and their correlated electrical PT100 reference sensors mounted used for the TV tests.
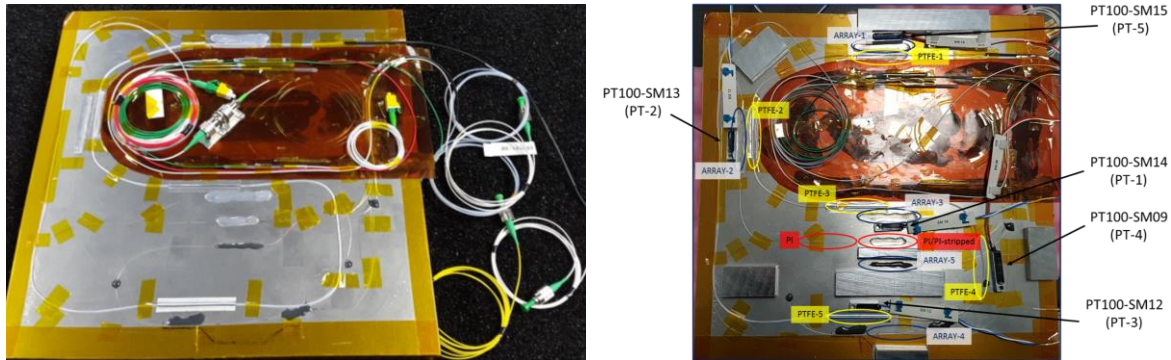
Figure 3. Panel with optical sensors installed (left). Panel with optical sensors and electrical PT100 reference sensors installed for TV tests (right).

For the atmospheric pressure test, a Votsch VT 7021 Temperature test chamber was used to cycle the temperature between -20°C and +80°C with the panel placed inside the chamber and the fibers exiting the chamber and connected to the FAZT I4_Bi interrogator. The FAZ I4_Bi interrogator was used to interrogate two PM-DTG fiber arrays where the individual sensors are mounted on the surface of the test panel. The FAZ I4_Bi interrogator was scanning the laser at 1kHz and continuously recording the data that was filtered and down-sampled to 10Hz.

Table 1. List of optical sensors and corresponding electrical reference for TV tests

Sensor number	Optical Sensor	Electrical Reference
1	PTFE-1 (RTV)	PT-5
2	PTFE-2 (RTV)	Avg(PT-1, PT-2)
3	PTFE-3 (ALU)	PT-3
4	PTFE-4 (Loose)	Avg(PT-1, PT-3, PT-4)
5	PTFE-5 (ALU)	PT-3
6	ARRAY-2 (RTV)	Avg(PT-2, PT-5)
7	ARRAY-3 (RTV)	Avg(PT-3, PT-5)
8	ARRAY-4 (Loose)	PT-3

Figure 4 shows a photo of the full Thermal Vacuum setup (left) and a photo of the panel sandwiched between the heating/cooling plates (right). The TV chamber had the following dimensions 500×500mm and is equipped with an N2 cooler (Cooling Plate 340×340mm² and electric heaters). Temperatures between -80°C and +125°C can be approached. The chamber was equipped with a Leybold Trivac 16 pump and a 255 Edwards turbo pump. With this, pressures down to P<2E-6mbar can be achieved. The DAQPRO 5300 data logger was used to monitor $5 \times$ PT100 sensors installed on the panel and were used as a measurement reference point for each temperature measurement.
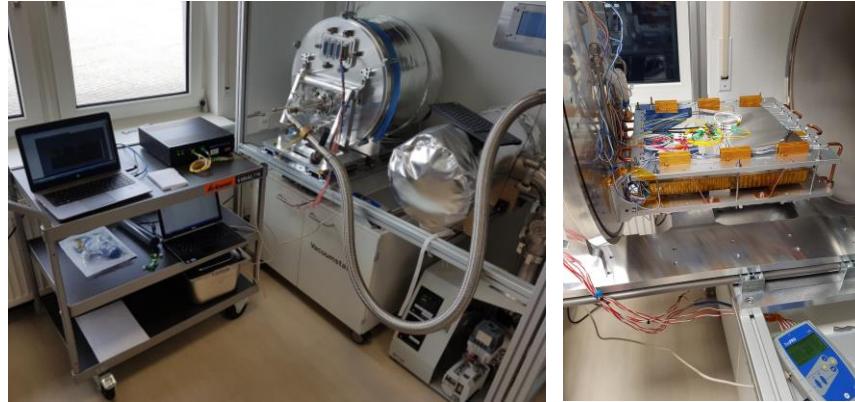
Figure 4: TV test setup (left), test panel sandwiched between heating/cooling plates in the TV chamber (right)

3. SENSOR CALIBRATION

PM-FBGs (or Bi-FBGs) have a double Bragg peak that enables the simultaneous measurement of strain (ε) and temperature (T). This is often at the expense of the measurement accuracy due to the decoupled sensitivities being small. The PM-DTG from FBGS is based on draw tower gratings (DTGs) written in a Polarization Maintaining (PM) fiber. From temperature and strain calibrations, it is known that the response of the double peak with respect to strain is different compared to the response to temperature. In this way, the FBGs written in PM-fiber can discriminate to a large extent between strain and temperature. A typical reflection spectrum of a PM-DTG is shown in figure 5. The wavelength separation between two orthogonal peaks is around 0.6nm at room temperature[6, 7].
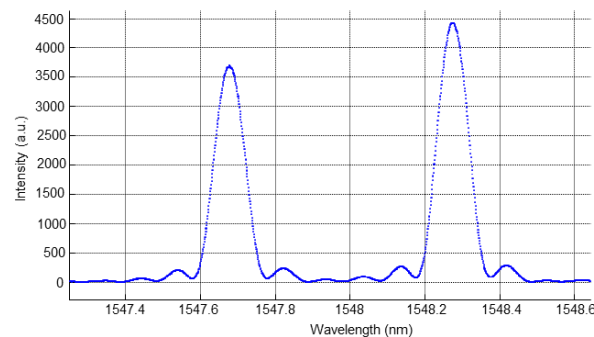
Figure 5. Typical reflection spectrum of PM-DTG

The response of the individual wavelengths λ_1, λ_2 to ε and T variations is very similar to the response for regular FBGs but there will be slight differences in sensitivity between the two peaks. Mathematically, we get a set of two equations that relate λ_1, λ_2 to ε and T with coefficients that are slightly different[6, 7] as shown in equations 1 and 2.

$$\lambda_1 - \lambda_{10} = a\ \Delta T + b\ \Delta\varepsilon \qquad (1)$$

$$\lambda_2 - \lambda_{20} = c\ \Delta T + d\ \Delta\varepsilon \qquad (2)$$

In equations (1) and (2), λ_1 is the low wavelength peak and λ_2 the high wavelength peak for the PM-FBG. The a, b, c and d parameters are the sensitivity parameters for strain ($\Delta\varepsilon$) and temperature (ΔT) and λ_{10} and λ_{20} are the reference wavelengths at known strain and temperature. The small differences in sensitivity originate predominantly from the temperature dependence of the stress birefringence, and the peak separation can be regarded as a direct measure for it. The sensitivity of the peak separation is a key parameter for the decoupling between ε and T. The inverse relation can be used to directly calculate the decoupled strain and temperature as shown in equations 3 and 4.

$$\Delta T = (d\Delta\lambda_1 - b\Delta\lambda_2)/D \qquad (3)$$

$$\Delta\varepsilon = (a\Delta\lambda_2 - c\Delta\lambda_1)/D \qquad (4)$$

Where $D = ad - bc$ is the determinant of the matrix.

For the 5× PM-DTG array factory calibration, a strain (0με → +2145με → 0με) and temperature (-20°C → +120°C → -20°C) calibration cycle was carried out using a FAZT I4_Bi interrogator to calculate the sensor sensitivities. The calibration coefficients can be obtained from calibrating each PM-DTG sensor, one sample PM-DTG sensor from an array, or an average of all PM-DTG sensors within an array. The average values of the strain/temperature sensitivities for the 5× PM-DTG arrays using linear calibration method are:

a = 11.48934 (pm/°C), c = 10.71543 (pm/°C), b = 1.123 (pm/με), d = 1.140 (pm/με)

The strain calibration setup was also used to evaluate the temperature error caused by induced strain when varied from 0 to 2145με with 10 steps up and 10 steps down as shown in figure 6 (left). The strain induced temperature error (peak to peak P2P) for the 5 × PM-DTG sensors using the above calibration coefficients was <1.1°C. Figure 6 (right) shows the strain induced temperature error (peak to peak P2P) for the 5 × PM-DTG array tested using the strain calibration setup when each individual sensor calibration was used to calculate the temperature error for all the other sensors in the same array in addition to using the average calibration coefficients for all sensors[5].

Calibration Set	avg cal	cal #1	cal #2	cal #3	cal #4	cal #5
Sensor #1	0.820	0.836	0.887	0.905	0.794	0.798
Sensor #2	0.674	0.597	0.754	0.783	0.626	0.653
Sensor #3	0.795	0.881	0.846	0.865	0.833	0.806
Sensor #4	0.727	0.856	0.649	0.667	0.798	0.750
Sensor #5	0.973	0.881	1.058	1.080	0.910	0.946
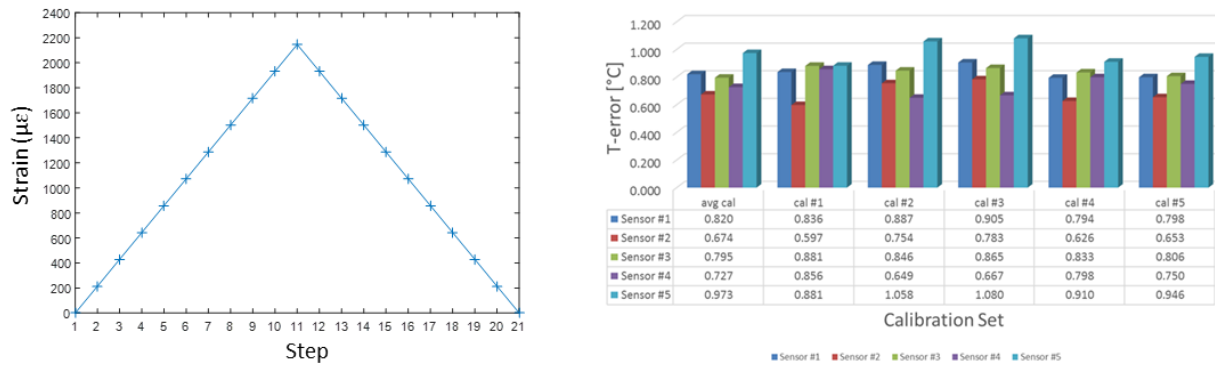
Figure 6. Linear longitudinal strain steps (0με → +2145με → 0με) applied to a 5 × PM-DTG (left). Induced temperature measurement error (P2P) for a calibrated 5 × PM-DTG array for the corresponding strain (0με → +2145με → 0με) using individual and average calibrated sensitivities (right)

An example of the temperature error of a PM-DTG temperature cycled in an oven from -20°C to +80°C is shown in figure 7 (left) using the standard linear calibration formula. The effects of non-linearity and hysteresis due to the coating is observed between -20°C and +20°C. By applying a quadratic post correction factor after the linear calibration formula calculation, the error can be reduced to <±1°C as shown in figure 7 (right). The hysteresis is expected to be due to the humidity effects on the coating[5].
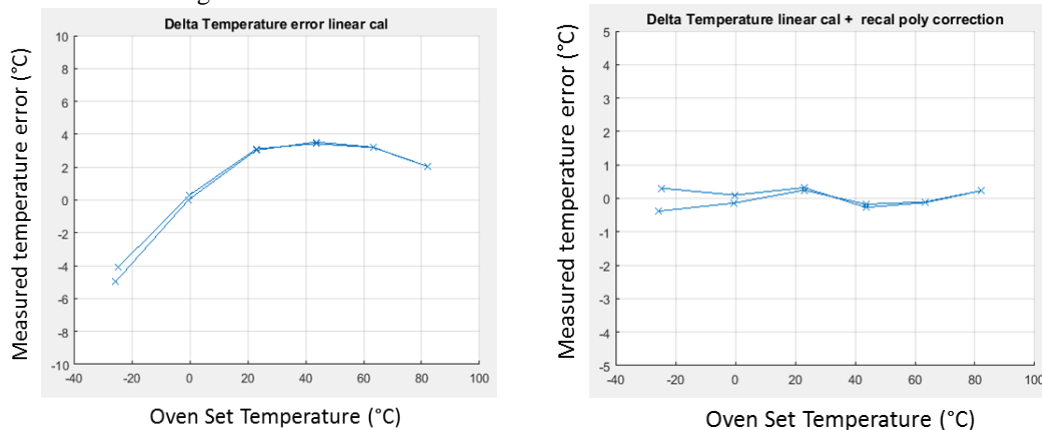
Figure 7. Temperature induced measurement error for a PM-DTG sensor in a 5 × PM-DTG array over a full temperature cycle (-20°C to +80°C to -20°C) (left). Temperature induced measurement error for a PM-DTG sensor using linear calibration + quadratic post correction (Right).

Since the temperature dependence is non-linear, it is possible to use a higher order polynomial to generate the calibration curves (e.g. quadratic or cubic) instead of assuming it is linear as shown in equation 3. This can be achieved by using the delta wavelength (dλ) and mean wavelength (Λ) parameters of the two orthogonal PM-DTG sensor peaks and their dependency on strain and temperature as shown in equation 5 and 6 instead of using equation 1 and 2.

$$\Delta d\lambda = a\ \Delta\varepsilon + b\ \Delta T^3 + c\ \Delta T^2 + d\ \Delta T + e \qquad (5)$$

$$\Delta\Lambda = f\ \Delta\varepsilon + g\ \Delta T^3 + h\ \Delta T^2 + i\ \Delta T + j \qquad (6)$$

where $\Delta d\lambda = \lambda_2 - \lambda_1$, $\Lambda = (\lambda_2 + \lambda_1)/2$, e=e1+e2 and j=j1+j2.

The relationship between $\Delta\lambda$ and Strain is linear (y= a*x+e2) and is used to calculate the coefficients a and e2 (y= $\Delta\lambda$, x= Strain). The relationship between Λ and Strain is also linear (y=f*x+j2) and is used to calculate the coefficients f and j2 (y= Λ, x= Strain). The relationship between $\Delta\lambda$ and temperature is cubic (y= $bx^3 + cx^2 + dx + e1$) and is used to calculate the coefficients b, c, d, and e1 (y= $\Delta\lambda$, x= Temperature). The relationship between Λ and temperature is also cubic (y= $gx^3 + hx^2 + ix + j1$) and is used to calculate the coefficients g, h, i, and j1 (y= Λ, x= Temperature).

Rearranging and substituting terms from equations 5 and 6 results in a cubic formula for ΔT as shown in equation 7.

$$aa\ \Delta T^3 + bb\ \Delta T^2 + cc\ \Delta T + dd\ = 0 \qquad (7)$$

where aa= (ag - fb), bb= (ah- fc), cc= (ai - fd), dd= (aj + fe + f $\Delta\lambda$ – a $\Delta\Lambda$)

Solving this equation will result in the temperature measurement. Figure 8 shows the temperature induced measurement error for a PM-DTG sensor in a 5×PM-DTG array tested using a cubic calibration formula. However, this approach requires more computation resources and complexity, therefore is not used in this paper.
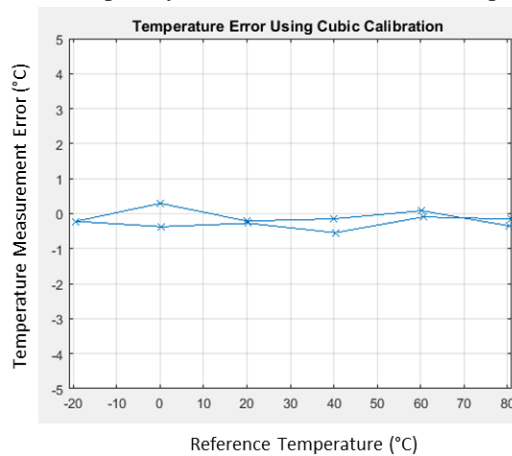
Figure 8. Temperature induced measurement error for a PM-DTG sensor using cubic calibration formula.

4. TEMPERATURE MEASURMENTS

The experiments in this paper will consist of measuring the temperature error of the PM-DTGs installed on a satellite test panel tested in a thermal chamber in an atmospheric pressure environment and thermal vacuum environment. The following four tests were carried out as shown in table 2. The first test was used for sensor calibration/correction. All the measurements in the paper will be based on the post corrected data based on the calibration information from the atmospheric 1st stage single temperature cycle measurements.

Table 2. Demonstrator experiments

Experiment	Description	Comments
1 (Atmospheric Pressure)	1st Single Temperature Cycle Test Sensor Calibration/Accuracy Test	1st stage calibration. 11 Steps @ 20°C/step (-20°C →80°C→ -20°C)
2 (Atmospheric Pressure)	Temperature Aging Test (10 cycles)	10 full cycles. Total of 2 steps @ 100°C (-20°C →80°C→ -20°C)
3 (Atmospheric Pressure)	2nd Single Temperature Cycle Test Sensor Accuracy Verification Test (Atmospheric Pressure environment)	Accuracy verification. 11 Steps @ 20°C/step (-20°C →80°C→ -20°C)
4 (Thermal Vacuum)	3rd Single Temperature Cycle Test Sensor Accuracy Verification Test (TV environment)	Accuracy verification. 11 Steps @ 20°C/step (-20°C →80°C→ -20°C)

4.1 First Single Temperature Cycle Test for Calibration– Atmospheric Pressure Environment

The test was performed with a full cycle containing temperature plateaus at -20°C, 0°C, +20°C, +40°C, +60°C, and +80°C as shown in figure 9. The constant plateau temperatures were stabilised for at least 30 minutes each. The MilliK high precision thermometer with the ISOTECH High precision electrical probe (935-14-61) was used as a measurement reference point at each step. The interrogator peak data was filtered and down sampled to 10Hz. The electrical data was sampled at a lower rate between 0.1-1Hz. Both the electrical and temperature data were aligned and synchronized based on their time stamps. When the oven temperature was stabilised at every temperature step, the electrical reference temperature measurement and optical peak wavelength for the optical sensors were recorded figure 9.
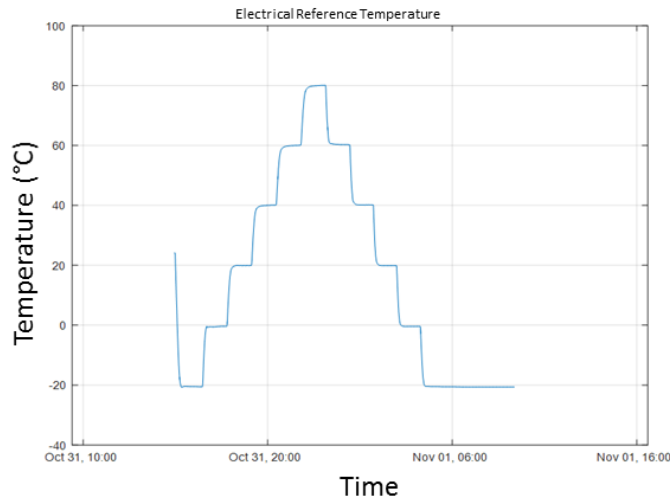
Figure 9: Electrical temperature reference for 1st single temperature cycle test in atmospheric pressure environment.

The optical wavelength for the detected two orthogonal peaks of sensor #1 (PTFE-1 (RTV)) are shown in figure 10 (left) and varied by ~1.2-1.3nm for a temperature change between -20°C and +80°C, while the delta wavelength between the two orthogonal peaks are shown in figure 10 (right) and varied between 652pm to 569pm (~83pm) for a temperature change between -20°C and +80°C. This highlights a difference in temperature sensitivity between the PM-DTG delta wavelength and the individual orthogonal peaks wavelength shift by at least an order of magnitude for a temperature change of 100°C.
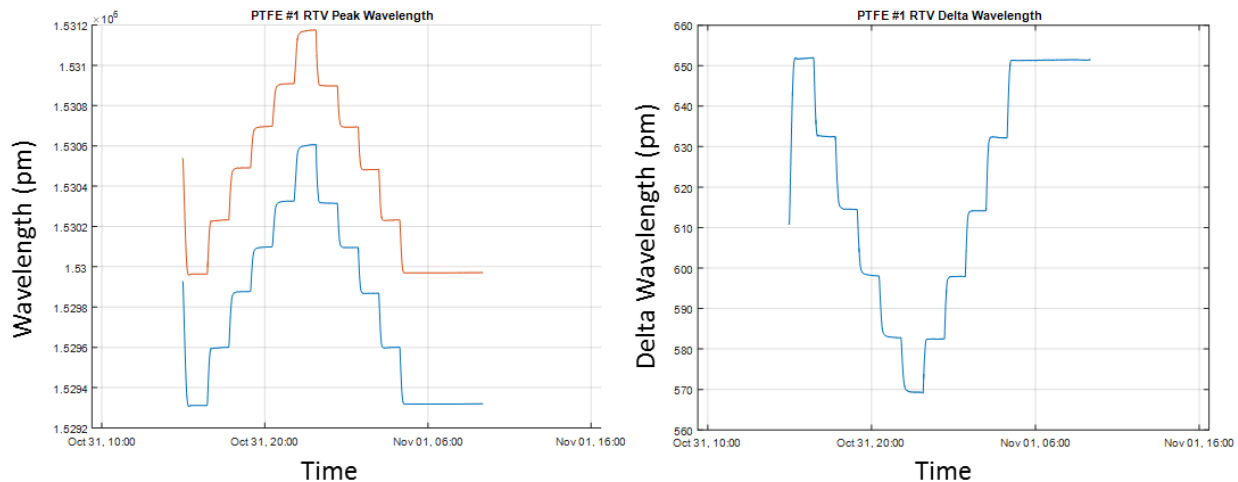
Figure 10: Optical PM-DTG sensor PTFE-1 (RTV) wavelength measurements for 1st single temperature cycle test individual orthogonal peaks (left), delta wavelength between the peaks (right) measured in atmospheric pressure environment.

Figure 11 and figure 12 show the residual temperature measurement error for a single temperature cycle test using linear calibration + quadratic (2nd order polynomial) post correction for the 5 × PM-DTG PTFE sensors (Sensor # 1-5) and 3 × PM-DTG Array sensors (Sensor # 6-8) respectively.
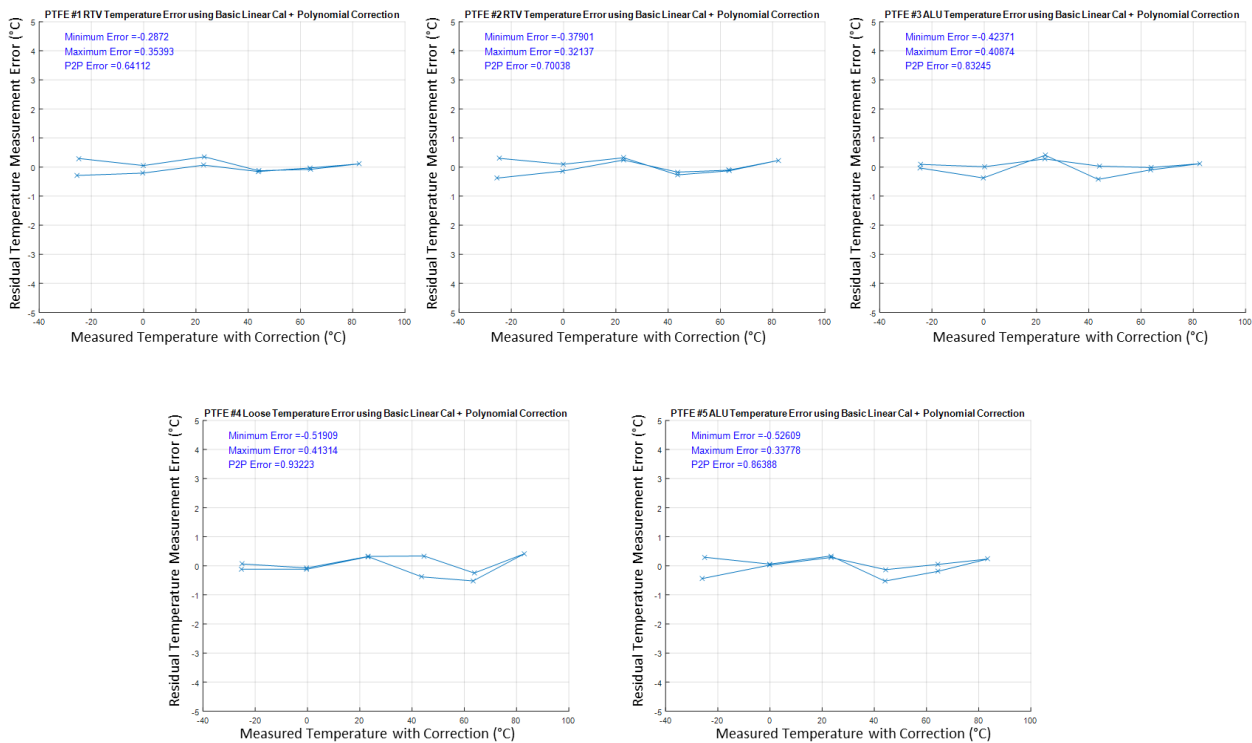
Figure 11: Residual temperature measurement error for 1st single temperature cycle test using linear calibration + quadratic (2nd order polynomial) post correction for the 5 × PM-DTG PTFE sensors in atmospheric pressure environment
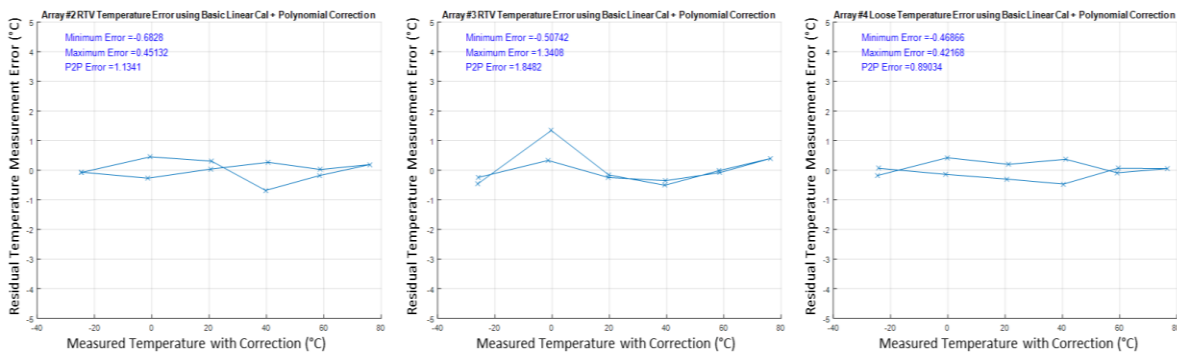
Figure 12: Residual temperature measurement error for 1st single temperature cycle test using linear calibration + quadratic (2nd order polynomial) post correction for the 3 × PM-DTG Array sensors in atmospheric pressure environment

A summary of the calculated residual errors for all 8 PM-DTG sensors are shown in figure 13. The residual error shows and peak to peak (P2P) error for each optical PM-DTG sensor when compared to the electrical reference sensor (MilliK high precision thermometer with the ISOTECH High precision electrical probe (935-14-61)).
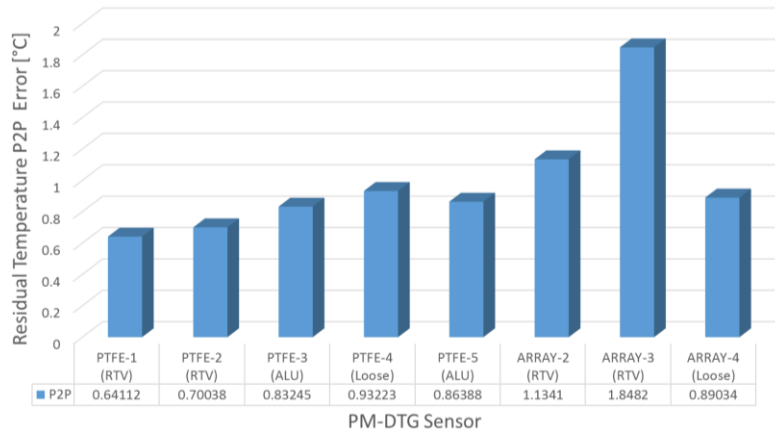
Figure 13: Residual P2P temperature measurement error for all PM-DTG sensors for 1st single temperature cycle test in atmospheric pressure environment

4.2 Multi Temperature Cycle Aging Test – Atmospheric Pressure Environment

To demonstrate the aging effects on the sensor in an Atmospheric Pressure thermal chamber, multiple temperature cycles were performed on the test panel by setting the temperature of the chamber to the lowest temperature point at -20°C, and then ramping the temperature up to +80°C and then back down to -20°C for at least 10 full cycles as shown in figure 14. The interrogator peak data for the optical sensors were filtered and down sampled to 10Hz. The MilliK high precision thermometer with the ISOTECH High precision electrical probe (935-14-61) was used as a measurement reference point at both extreme temperatures and was sampled at a lower rate between 0.1-1Hz. Both the electrical and temperature data were aligned and synchronized based on their time stamps. At the extreme temperatures set points -20°C, and +80°C, the temperatures were stabilised for at least 1.5 hour before ramping the temperature again. Figure 14 and figure 15 show the electrical and optical (linear calibration + quadratic 2nd order polynomial correction) temperature measurements for a 10 multi temperature cycle test for the 5 × PM-DTG PTFE sensors (Sensor # 1-5) and 3 × PM-DTG Array sensors (Sensor # 6-8) respectively using the derived coefficients from the first temperature calibration cycle.
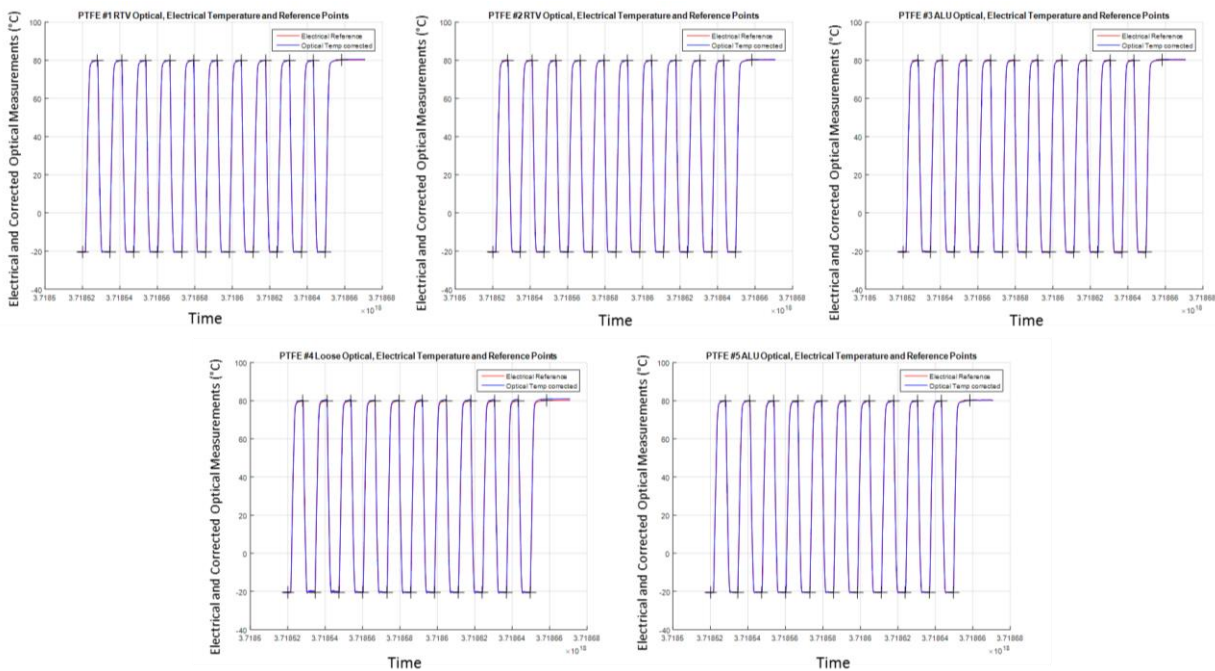
Figure 14: Electrical and optical temperature measurements (°C) for a multi temperature cycle test using linear calibration + quadratic post correction for the 5 × PM-DTG PTFE sensors in atmospheric pressure environment
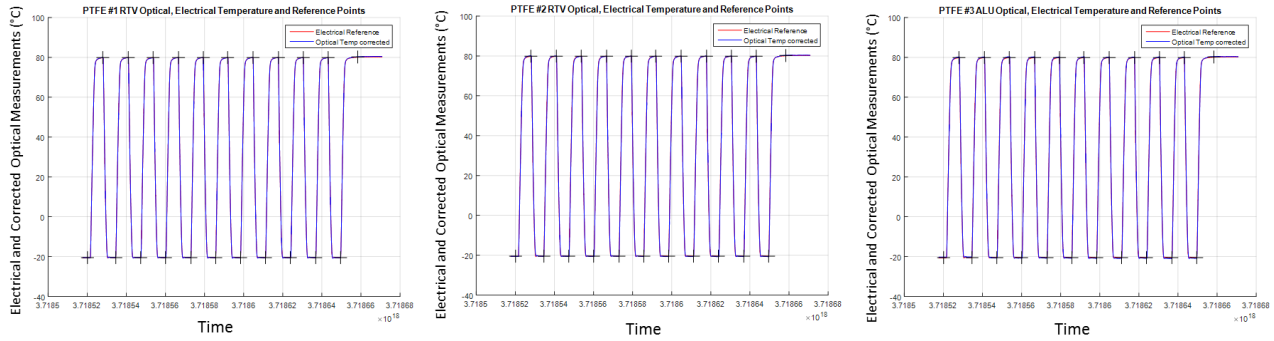
Figure 15: Electrical and optical temperature measurements (°C) for a multi temperature cycle test using linear calibration + quadratic post correction for the $3 \times$ PM-DTG Array sensors in atmospheric pressure environment

4.3 Second Single Temperature Cycle Test – Atmospheric Pressure Environment

This test was performed with a full single cycle similar to the 1st cycle containing temperature plateaus at -20°C, 0°C, +20°C, +40°C, +60°C, and +80°C after the 10 multi cycle test to evaluate the aging effects on the calibration of the sensors. The constant plateau temperatures were stabilised for at least 30 minutes each. The MilliK high precision thermometer with the ISOTECH High precision electrical probe (935-14-61) was used as a measurement reference point. The interrogator peak data was filtered and down sampled to 10Hz. The electrical data was sampled at a lower rate between 0.1-1Hz. Both the electrical and temperature data were aligned and synchronized based on their time stamps. Figure 16 and figure 17 show the residual temperature measurement error for the second single temperature cycle test using linear calibration + quadratic (2nd order polynomial) post correction for the $5 \times$ PM-DTG PTFE sensors (Sensor # 1-5) and $3 \times$ PM-DTG Array sensors (Sensor # 6-8) respectively using the derived coefficients from the first temperature calibration cycle.
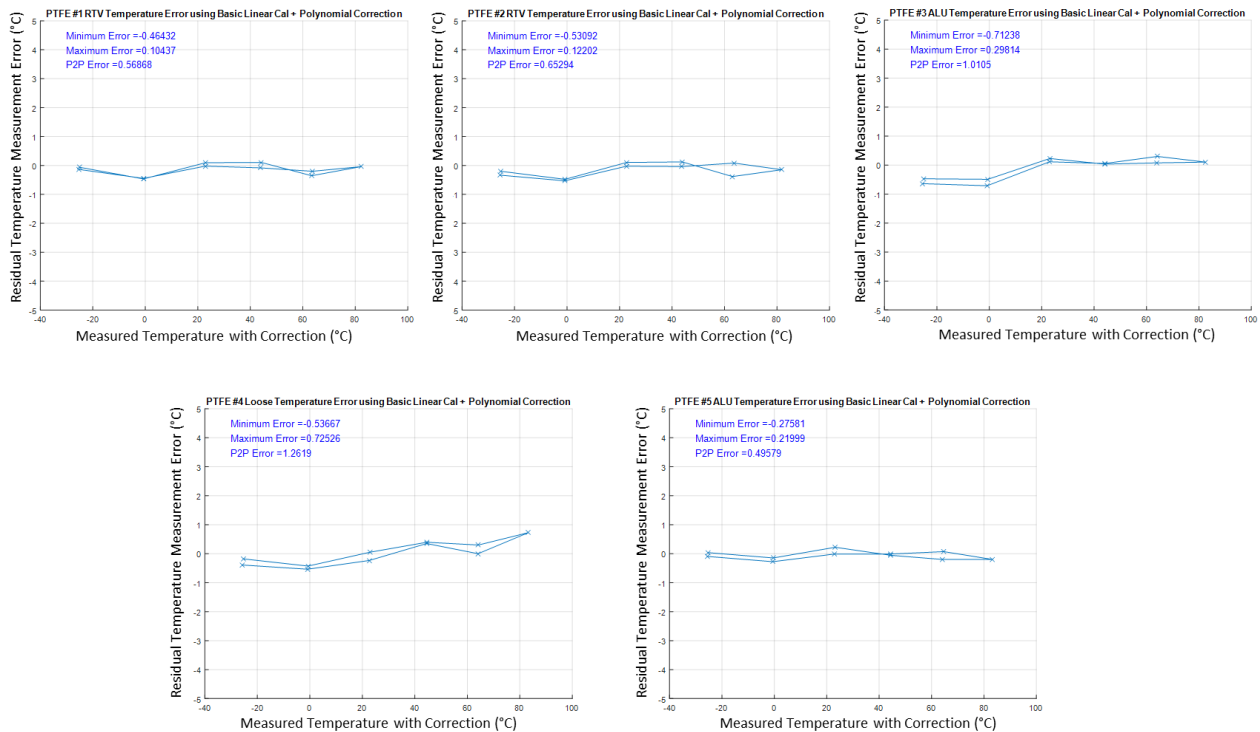
Figure 16: Residual temperature measurement error for 2nd single temperature cycle test using linear calibration + quadratic (2nd order polynomial) post correction for the $5 \times$ PM-DTG PTFE sensors in atmospheric pressure environment
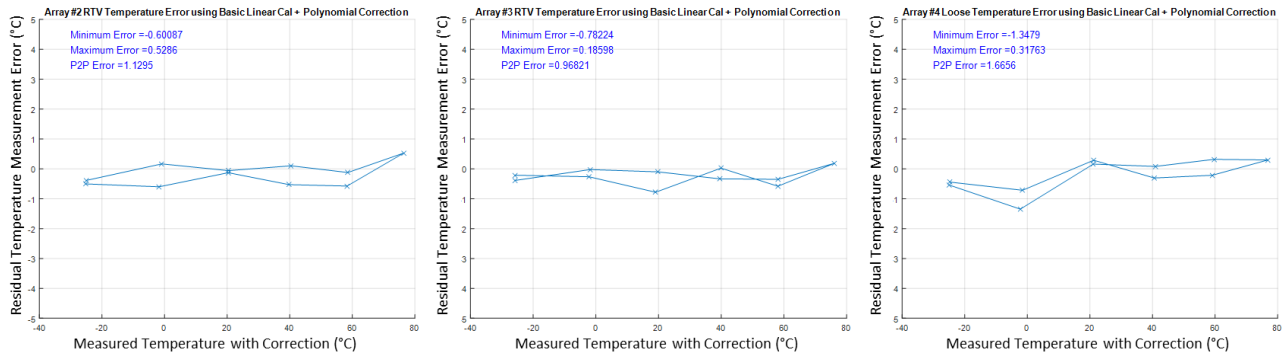
Figure 17: Residual temperature measurement error for 2nd single temperature cycle test using linear calibration + quadratic (2nd order polynomial) post correction for the $3 \times$ PM-DTG Array sensors in atmospheric pressure environment

A summary of the calculated residual peak to peak (P2P) errors for all the 8 PM-DTG sensors when compared to the electrical reference sensor (MilliK high precision thermometer with the ISOTECH High precision electrical probe (935-14-61)) are shown in figure 18.

PM-DTG Sensor	PTFE-1 (RTV)	PTFE-2 (RTV)	PTFE-3 (ALU)	PTFE-4 (Loose)	PTFE-5 (ALU)	ARRAY-2 (RTV)	ARRAY-3 (RTV)	ARRAY-4 (Loose)
P2P	0.56868	0.65294	1.0105	1.2619	0.49579	1.1295	0.96821	1.6656
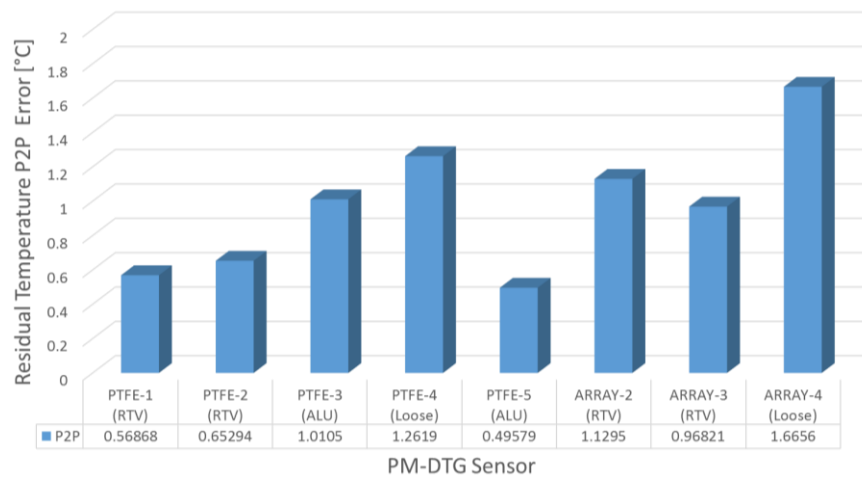
Figure 18: Residual P2P temperature measurement error for all PM-DTG sensors for 2nd single temperature cycle test in atmospheric pressure environment

4.4 Third Single Temperature Cycle Test – TV Environment

This test was performed in a thermal vacuum environment with a full cycle containing temperature plateaus at -23°C, 0°C, +20°C, +40°C, +60°C, and +82°C. The extreme temperatures -23°C and +82°C set points were used instead of -20°C and +80°C due to a temperature offset observed between the controller temperature PT100 sensors and the PT100 sensors installed on the panel and guarantee that the panel temperature will experience -20°C and +80°C. The constant plateau temperatures were stabilized for at least 60 minutes each. The heating steps would reach stable temperatures within 2 hours while the cooling steps required at least 6 hours before stabilizing as shown in figure 19. Five PT100 electrical sensors were installed on the panel and connected to the DAQPro data acquisition system.

The selection of PT100 sensors used as an electric reference versus the optical sensors are shown in table 1. The Thermal Vacuum system maintained a pressure <=3.1E-5 throughout the measurements. The interrogator peak data was filtered and down sampled to 10Hz. The electrical data was sampled at a lower rate at 0.1Hz. Both the electrical and temperature data were aligned and synchronized based on their time stamps.
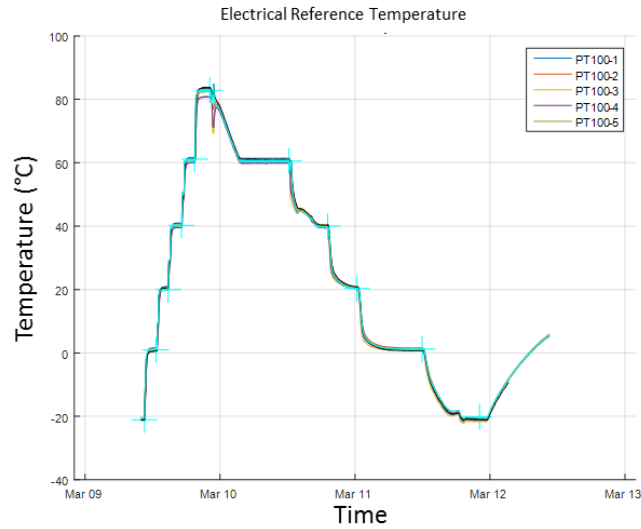
Figure 19: Electrical temperature reference sensors PT100 for 3rd single temperature cycle test in TV environment

Figure 20 and figure 21 show the residual temperature measurement error for the 3rd single temperature cycle test in TV environment using linear calibration + quadratic (2nd order polynomial) post correction for the $5 \times$ PM-DTG PTFE sensors (Sensor # 1-5) and $3 \times$ PM-DTG Array sensors (Sensor # 6-8) respectively using the derived coefficients from the first temperature calibration cycle.
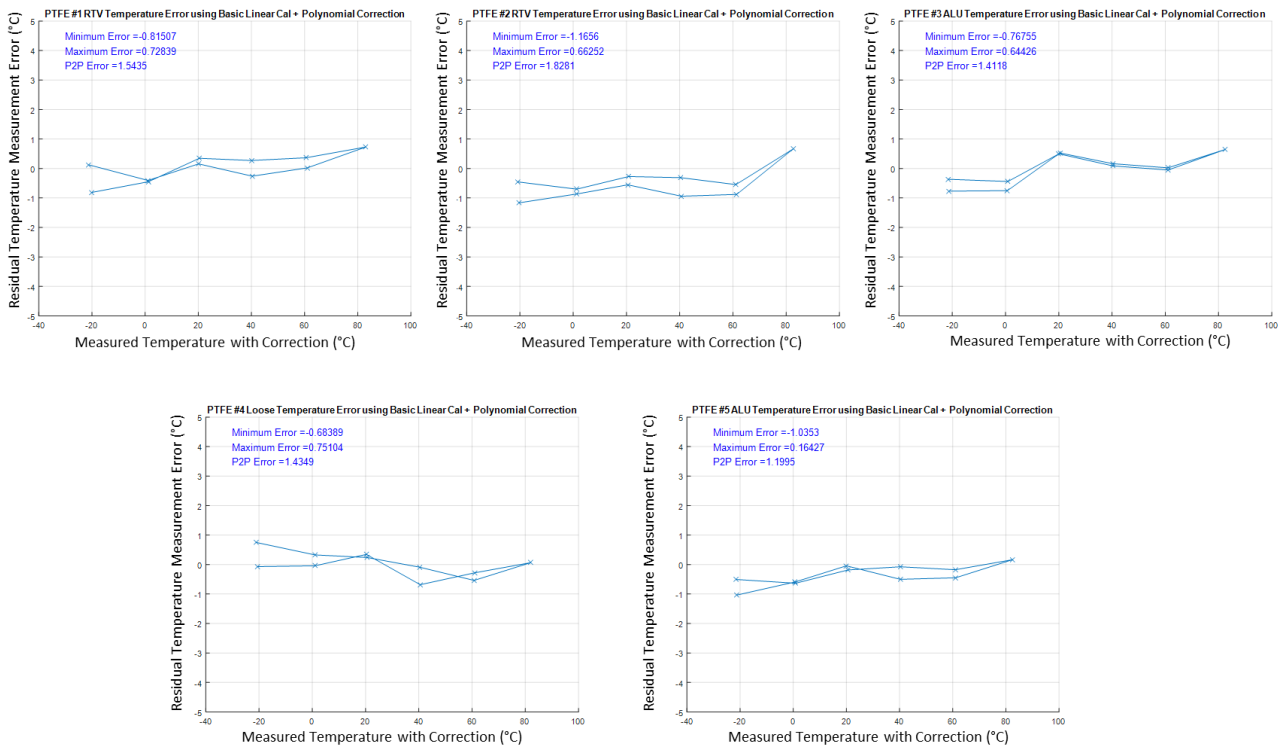
Figure 20: Residual temperature measurement error for 3rd single temperature cycle test using linear calibration + quadratic post correction for the $5 \times$ PM-DTG PTFE sensors in TV environment
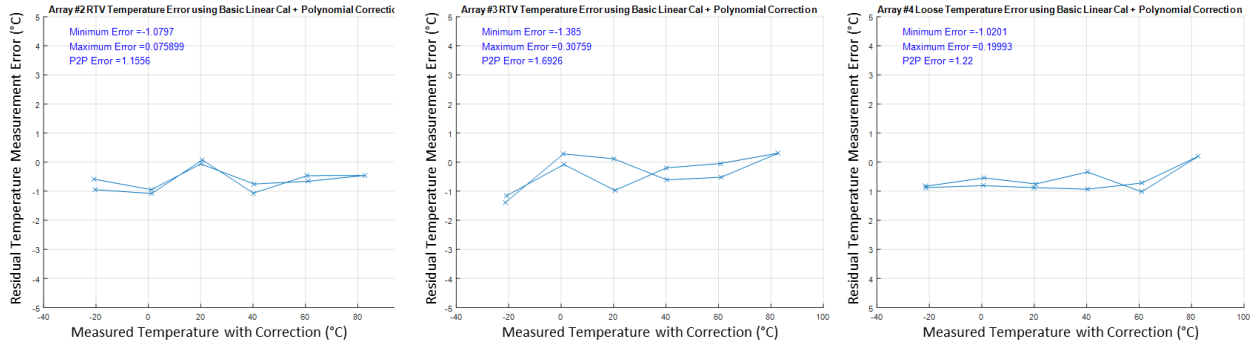
Figure 21: Residual temperature measurement error for 3rd single temperature cycle test using linear calibration + quadratic post correction for the $3 \times$ PM-DTG Array sensors in TV environment

A summary of the calculated residual P2P errors for all 8 PM-DTG sensors when compared to the electrical PT100 sensors is shown in figure 22.
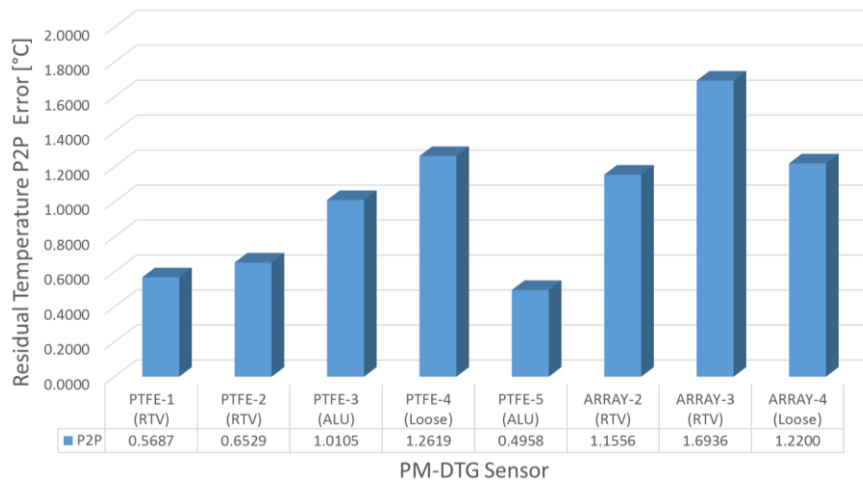
Figure 22: Residual P2P temperature measurement error for all PM-DTG sensors for 3rd single temperature cycle test using linear calibration + quadratic (2nd order polynomial) after correction in TV environment

5. CONCLUSIONS

We have developed an optical sensing system that can interrogate birefringent FBGs (PM-FBG) enabling simultaneous measurement of strain and temperature or perform strain independent temperature measurements. Two PM-DTG sensor arrays with PTFE, RTV, and Loose mounting techniques, were used to demonstrate a temperature measurement system for satellite test panels that can be used to simplify AIT, and can work in normal ground conditions at atmospheric pressures and in vacuum conditions. The system demonstrated <1°C induced error when the PM-DTG sensor array was exposed to strain up to 2145με. The temperature accuracy error varied between 0.5°C and 1.7°C peak to peak over -20°C and 80°C temperature range, in both atmospheric pressure environment and thermal vacuum environments.

ACKNOWLEDGEMENTS

REFERENCES

[1] Hurni, A., Lemke, N.M.K., Roner, M., Obermaier, J., Putzer, P., Kuhenuri, N., "Fiber-Optical Sensing On-Board Communication Satellites," In Proc. International Conference on Space Optics ICSO 2014, 2014.

[2] Ibrahim, S.K., Honniball, A., McCue, R., Todd, M., O'Dowd, J.A., Sheils, D., Voudouris, L., Farnan, M., Hurni, A., Putzer, P., Lemke, N., Roner, M., "Design Challenges of a Tunable Laser Interrogator for Geo-Stationary Communication Satellites", International Conference on Space Optics ICSO 2016, Paper 153, 2016.

[3] Putzer, P., Hurni, A., Ziegler, B., Panopoulou, A., Lemke, N., Costa, I., Pereira, C., "Photonically Wired Spacecraft Panels – An Economic Analysis and Demonstrator for Telecommunication Satellites", International Conference on Space Optics (ICSO), Paper 215, 2016

[4] Ibrahim, S.K., O'Dowd, J.A., McCue, R., Honniball, A., Farnan, M., Karabacak, D.M., Van Roosbroeck, J., Van Hoe, B., Vlekken, J., Lindner, E., Singer, J.M., "Ground Testing of Satellite Structures using Optical PM-FBG Sensors to Simultaneously Measure Strain and Temperature", 14th European Conference on Spacecraft Structures Materials and Environmental Testing (ECSSMET 2016), Paper A56173SI, 2016.

[5] Ibrahim, S.K., McCue, R., O'Dowd, J.A., Farnan, M., Karabacak, D.M., "Fiber Sensing for Space Applications", European Conference on Spacecraft Structures Materials and Environmental Testing (ECSSMET 2018), 2018.

[6] Van Roosbroeck, J., Ibrahim, S.K., Lindner, E., Schuster, K. and Vlekken, J., "Stretching the Limits for the Decoupling of Strain and Temperature with FBG based sensors," International Conference on Optical Fibre Sensors (OFS24), 96343S-96343S, 2015.

[7] Ibrahim, S.K., Van Roosbroeck, J., O'Dowd, J., Van Hoe, B., Lindner, E., Vlekken, J., Farnan, M., Karabacak, D.M., Singer, J.M., "Interrogation and mitigation of polarization effects for standard and birefringent FBGs," SPIE Commercial+Scientific Sensing and Imaging, Fiber Optic Sensors and Applications XIII, 98520H, (2016).